JOURNAL OF AIRCRAFT
Vol. 33, No. 3, May–June 1996

Launch Vehicle Acoustics Part 1: Overall Levels and Spectral Characteristics

S. A. McInerny*
University of Alabama, Tuscaloosa, Alabama 35487-0276

Far-field acoustic data measured during a series of launches are summarized. Comparisons of measured overall sound pressure levels (OASPLs) with predictions using an acoustic efficiency factor of 0.5% suggest that small thrust engines may have lower efficiency factors and high thrust engines may have higher efficiency factors. Directivity factors derived from vertical launch data measured during the 1950s are shown to better predict the timing and rate of rise and fall in far-field OASPLs than do the more widely used directivity factors derived from horizontally fired rocket data. Nonlinear propagation effects are believed to contribute to the decrease in peak low-frequency levels that control the OASPL and to increase the higher frequency levels, whereas atmospheric absorption decreases the high-frequency levels. Dimensionless constant bandwidth (narrow-band) sound power spectral densities (PSDs) estimated from measured sound pressure spectral densities are presented for the Peacekeeper, Delta, Scout, and Titan IV. Similarities and differences between these PSDs and a widely utilized PSD based on one-third-octave band sound pressure levels (OBSPLs) measured during the late 1950s and the 1960s are noted.

Nomenclature

C_e = speed of sound in exhaust at nozzle exit plane
D_e = engine exit diameter
D_{eq} = equivalent engine exit diameter for closely clustered engines
d = distance from launch pad to observer
f = frequency, Hz
L_c = laminar core length
L_s = supersonic core length
M_e = nozzle exhaust Mach number, V_e/C_e
PSD(f) = dimensionless sound power spectral density
$p'^2(f)$ = sound pressure spectral density, pressure squared per Hz
$Q(\theta)$ = overall sound pressure directivity factor
$q(f, \theta)$ = frequency dependent directivity factor
R = distance from source to observer
T = engine thrust
V_e = exhaust velocity at nozzle exit plane
W_m = engine mechanical power, $\frac{1}{2}TV_e$, approximate when imperfectly expanded
η = acoustic efficiency factor
θ_p = peak directivity angle
$\rho_0 c_0$ = characteristic acoustic impedance in air
$\langle\ \rangle$ = time average

Introduction

OVER the last 10 years, the author has collected and reviewed far-field rocket noise measurements made by a number of different organizations using a variety of instrumentation systems. One of the first sets of data reviewed was a series of measurements made at six microphone locations (3.32–18.35 km from the pad) during three launches of a Titan IIID vehicle during the mid-1970s. These (unpublished) data sets were studied at length in connection with the development of a noise prediction scheme for proposed Advanced Launch System vehicle designs. In comparing the Titan IIID data sets to estimates made using established prediction procedures, it was noted that the octave band sound pressure level (OBSPL) data measured at six locations during the three different launches displayed a trend of anomalously low absorption at high frequencies.

Several years ago, a set of measurements was made during the launch of a Titan IV. More recently, a series of acoustic measurements was made during launches of three different, smaller rockets and another Titan IV. The first of the smaller rockets was a Peacekeeper missile with a thrust of 2.2 MN. The second was a Delta vehicle, which has nine strap-on solid fuel engines around the core of the vehicle. Adjacent pairs of engines are lit on the ground with a single unlit engine between each pair, providing a total of six solid engines firing at liftoff. Including the liquid core engine, Delta's total liftoff thrust is 3.1 MN. The third was a Scout, which has a single solid rocket engine with a liftoff thrust of 0.44 MN. The Titan IV has a thrust of 10.5 MN.

In this article, analyses of these more recent data sets are presented. A background section is provided to clarify the relevant source characteristics and the source-receiver geometry during the launch. Analyses of far-field data recorded during the Titan IV, Peacekeeper, Delta, and Scout launches are then summarized in the form of maximum overall sound pressure levels, dimensionless one-third-OBSPLs and constant bandwidth (BW) PSDs. Predictions of OASPLs vs time are compared to measured data, and it is shown that the predictions are improved by the use of directivity factors derived from vertical launch. Normalized one-third-OBSPLs and dimensionless sound power spectral densities (PSDs) are also presented. These display high-frequency levels that decrease with distance less than expected on the basis of atmospheric absorption and spherical spreading, consistent with the trend first seen in the Titan IIID data.

Background

Undeflected Rocket Plume

Dominant Sound Source Region

The length of the laminar core in a rocket plume is estimated to be between 16–20 nozzle exit diameters D_e (Ref. 1). The region in a rocket exhaust, within which the flow remains supersonic, defines the supersonic core. This region is estimated to extend over a length of 25–35 exit diameters downstream of the nozzle exit plane.[1–4] Typical rocket nozzle exhaust Mach

Received Sept. 1, 1994; revision received Jan. 5, 1996; accepted for publication Jan. 6, 1996. Copyright © 1996 by the American Institute of Aeronautics and Astronautics, Inc. All rights reserved.

*Associate Professor, Department of Mechanical Engineering, P.O. Box 870276. Member AIAA.

numbers are in the range of $3.0 \leq M_e \leq 3.5$. Because of the high temperature of a rocket exhaust (1800–2100 K), flow in the dominant sound source region that is subsonic with respect to the speed of sound in the plume remains supersonic with respect to the atmosphere. Mach wave radiation and the extended length of the sound source region contribute to the high radiation efficiency of rockets.

A careful review of supersonic jet and small rocket noise studies indicates that the dominant sound source region in a rocket plume is centered somewhat downstream of the laminar core tip, but upstream of the tip of the supersonic core. A reasonable estimate for the length of this source region is the average of the lengths of the laminar and supersonic cores $(L_c + L_s)/2$.

Peak Directivity Angle

In a study of the noise radiated by rocket plumes, Cole et al.[5] found the angle of peak directivity for horizontally fired rockets to be between $50 < \theta_p < 60$ deg (relative to the downstream exhaust axis), whereas vertical launch data indicated peak radiation angles of $70 < \theta_p < 80$ deg. Cole et al. suggested four possible explanations for the larger directivity angles derived from vertical launch data. These included changes in source characteristics caused by vehicle motion, shortcomings in the procedure used to derive directivity factors from the launch data, effects induced by blast deflectors, and interaction of the launch noise with the ground. Based on the measured data, none of these explanations was considered satisfactory. In their report, Cole et al.[5] stated "No attempt is made in this report to give an explanation for these forward shifted directivity patterns."

There is another way to view the discrepancy between the directivity factors deduced from vertical launch data and those calculated from horizontal (plume axis parallel to the ground) test data: the horizontal ground test data are influenced by ground effects. This is an opinion based on data reviewed by the author, including data presented in this article and the data of Ref. 6. The latter reports the findings of a study on the effects of blast deflectors on liftoff noise. Of particular interest was the effect of blast deflectors on the vehicle acoustic loads. Different deflector configurations were studied as well as various nozzle exit-to-impingement surface distances. All of the tests were performed with horizontally fired model rockets. The deflectors were vertical and angled so that the deflected flow remained parallel to the ground. The data of Ref. 6 fail to reveal patterns consistent with expected behavior; in some cases higher on vehicle SPLs were measured on the side of the rocket away from the deflected plume. A comparison of blast deflector effects measured in Ref. 6 with those measured in scale model rocket deflector tests with vertical firings[7] and with those seen in launch data suggests that there are significant ground effects in acoustic data obtained from horizontally fired rocket tests.

Vertical Launch Considerations

For an observer location to be in the geometric far field, the distance from the source to the receiver must be much greater than the source dimensions. The length of the dominant sound source region in the plume has been estimated to be $(L_c + L_s)/2$. Thus, observer locations at distances $d >> 30D_e$ are considered to be in the geometric far field.

Radiation to the far field during a launch can be treated as that because of an undeflected plume when the predominant source region no longer impinges on the ground. During a launch, far-field OASPLs reach their maxima when the cone of maximum directivity (defined by the solid angle θ_p measured from the exhaust axis) passes over the measurement location. The required height of the nozzle from the ground for the radiation during this time period to be considered as that of an undeflected plume is estimated to be somewhat less than 1.5 times the supersonic core length, i.e., $h = 1.5L_s$ (see Fig. 1). Using an estimate of $L_s = 30D_e$ for the supersonic core length, the corresponding minimum distance from the pad to the observer for radiation to be treated as that caused by an undeflected plume is $d = 45D_e \tan \theta_p$ (assuming a vertical launch). With a peak directivity angle of $\theta_p = 70$ deg, this distance is about $d = 125D_e$.

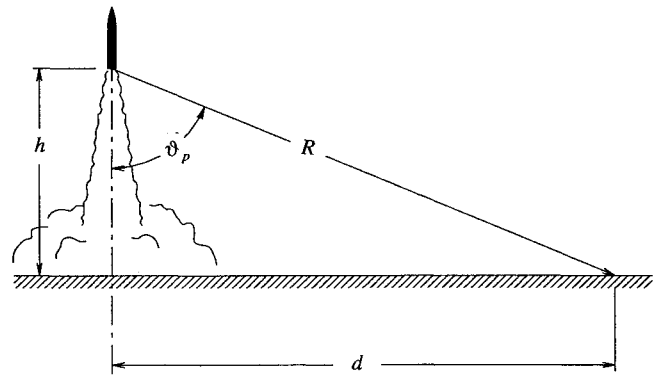

Fig. 1 Relationship between cone of maximum directivity (defined by solid angle θ_p), vehicle height h, distance from launch pad d, and source to receiver distance R.

With the exception of the first set of Titan IV data, sound power estimates and sound pressure predictions have been based on the assumption of a vertical launch trajectory. This is considered to be a good approximation for observer locations up to $2000D_e$ from the pad. For a peak directivity angle of $\theta_p = 70$ deg, the cone of maximum directivity (during the vertical portion of the ascent) intersects the ground in a circle of radius $2000D_e$ when the vehicle is at an altitude of $750D_e$.

Data Acquisition and Processing

Instrumentation Systems and Measurement Locations

First Titan IV Measurements

For the first set of Titan IV measurements, data were recorded at ground locations 0.5, 12.62, 13.58, and 15.73 km from the pad. The three distant measurement locations were all within a pie-shaped sector of a 9-deg arc angle (as measured on the ground from an origin at the launch pad), and at distances such that peak measured levels, assuming spherical spreading, would be expected to vary by no more than 2 dB from location to location. Two different instrumentation systems were used to measure the first set of Titan IV data. At the two measurement locations 150 nozzle diameters from the pad, Endevco model 2510 high-intensity piezoelectric microphones were used. Sound pressures were recorded on an FM tape recorder with an upper frequency limit of 2500 Hz. One-third-OBSPLs were calculated only for frequency bands from 8 to 2000 Hz. At the three locations 12.6–15.7 km from the pad, SPLs were measured using Bruel & Kjaer model 2143 real-time analyzers with model 4165 microphones. One-s-averaged one-third-OBSPLs were recorded to floppy disk at 1.0-s intervals. Measurement times were coordinated with launch times. In this article, these data sets are compared to predictions of OASPL vs time calculated using an established procedure.[8]

Recent Peacekeeper, Delta, Scout, and Titan IV Launch Measurements

In this series of measurements, data were recorded at locations 0.3, 0.61, and 1.22 km from the Peacekeeper pad; at locations 0.46, 0.61, and 0.92 km from the Delta pad; at locations 0.36, 0.64, 0.94, and 1.22 km from the Scout pad; and at locations 0.82, 2.04, 3.41, 5.79, and 13.15 km from a Titan IV pad. Bruel & Kjaer model 2230 sound level meters (SLMs) with model 4155 microphones were used to make this series of measurements. The frequency response of each SLM was measured exclusive of the microphone. Typically, the SLM

response was 1.0 dB down at frequencies from 3.5 to 7 Hz and down 3.0 dB at frequencies from 2 to 3.5 Hz. For the SLM at the second Delta measurement location, the 1.0-dB down frequency was 22 Hz and the 3.0-dB down frequency was 4.5 Hz. Calibration curves provided with the model 4155 microphones only extend down to 20 Hz. The Bruel & Kjaer catalog states that the 4155 microphone is acoustically similar to the 4165, which is nominally 1.0 dB down at 5 Hz and 3.0 dB down at 2 Hz.

For the Peacekeeper and Delta vehicles, peak one-third-OBSPLs were in the 50–80-Hz range. For the smaller Scout vehicle, peak one-third-OBSPLs were in the 100–125-Hz range. Peak one-third-octave band levels for these vehicles should not have been affected by low-frequency instrumentation roll-off. The peak frequency in the one-third-OB spectra of the Titan IV is close to 20 Hz; one-third-OBSPLs below this peak may have been affected by instrumentation roll-off. Measurement times were not coordinated with launch times in this series of measurements.

Dimensionless Parameters

Rocket noise data are presented in several forms in this article. Sound power estimates are given in the form of dimensionless PSDs for the Peacekeeper, Delta, Scout, and Titan IV. Dimensionless as well as raw one-third-OBSPLs are presented for the first set of Titan IV measurements. Procedures followed to cast the data in dimensionless form are detailed next.

Dimensionless Frequency

Sound power spectral densities estimated from measured SPLs are presented as a function of Strouhal number fD_e/V_e. Using this form of the dimensionless frequency, constant bandwidth PSDs peak at a Strouhal number close to 0.025 (Ref. 8). (This dimensionless frequency is an order of magnitude lower than that of the peak in subsonic jet PSDs, as discussed in Refs. 1 and 3.)

When a vehicle has multiple clustered engines, an equivalent diameter is generally used to calculate the dimensionless frequency.[4] For n identical, closely clustered engines with nozzle exit diameters D, the equivalent single engine diameter is taken to be $D_{eq} = \sqrt{nD^2}$. The Peacekeeper and Scout vehicles have single engines, so that D_{eq} is simply the diameter at the nozzle exit plane. The two Titan IV engines are well separated, so that the value of D_{eq} taken for this vehicle was the exit diameter of a single engine. Because the Delta's six ignited (during liftoff) solid engines are clustered in pairs separated by a single unlit engine, an equivalent exit diameter of $\sqrt{2}D_e$ was used to calculate the Strouhal number for this vehicle. The Delta vehicle also has a liquid core engine that provides roughly a fifth of the vehicle's liftoff thrust. While included in the calculation of overall sound power, the effect of this core engine (which is shielded by the plumes of the strap-on solids), on the frequency distribution was assumed to be negligible.

Dimensionless PSDs

Assuming statistically stationary data, spherical spreading, and an observer in the geometric far field, the sound pressure spectral density $p'^2(R, f, \theta)$, can be expressed in terms of PSD(f) as

$$\frac{p'^2(R, f, \theta)}{\rho_0 c_0} = \frac{1}{4\pi R^2} q(f, \theta) \left[\left(\eta \frac{1}{2} TV_e\right) \mathrm{PSD}(f) \frac{D_e}{V_e}\right] \quad (1)$$

where the symbols and variables are as defined in the Nomenclature section.

Note that Eq. (1) does not account for an increase in sound pressure because of the ground reflection at the observer locations. The effect of ground reflections may have been incorporated into the larger peak directivity factors derived from vertical launch data in Ref. 5. The PSD(f) cannot be estimated from launch data using Eq. (1) without further approximation, because 1) the $q(f, \theta)$ is not known and 2) measured SPLs and spectral densities vary with time because of the motion of the vehicle. Hence, dimensionless sound power spectral densities were estimated from sound pressure spectral densities by averaging the sound pressure spectra over the time that the OASPL was within 6 dB of its maximum and by approximating the directivity factor as constant across all frequencies during this time period:

$$\frac{\langle p'^2[R(t), f, \theta(t)]\rangle}{\rho_0 c_0} = \frac{1}{4\pi R^2} Q(\theta) \left[\left(\eta \frac{1}{2} TV_e\right) \mathrm{PSD}(f) \frac{D_e}{V_e}\right] \quad (2a)$$

or

$$\text{dimensionless PSD}(f) = \frac{\langle p'^2[R(t), f, \theta(t)]\rangle}{\rho_0 c_0} \frac{4\pi R^2}{(\eta \frac{1}{2} TV_e)} \frac{V_e}{D_e} \frac{1}{Q(\theta)} \quad (2b)$$

In the previous equations are the following:

1) Fast Fourier transform (FFT) calculations of the sound pressure at each measurement location were averaged over the time during which the (1-s averaged) OASPL was within 6 dB of the maximum. This time period was typically 7–13 s for the Peacekeeper, Delta, and Scout data locations, and 12–36 s for the Titan IV data sets. A Hanning window and 50% overlap processing were employed in the FFT calculations. Sound pressure spectral densities are presented in BWs of 4 Hz in the frequency range from 0 Hz up to a frequency corresponding to $fD_e/V_e \approx 0.1$, a BW of 20 Hz between $0.1 \leq fD_e/V_e \leq 1.0$, and a BW of 100 Hz over the remainder of the high-frequency range.

2) At any measurement location, the rapid increase and decrease in OASPLs during the period of maximum acoustics is controlled primarily by the changing angle of directivity. Using the Cole et al.[5] vertical launch data, one can estimate peak overall directivity factors of 7 to 8 dB. Since a 6-dB down-averaging period was used, during which the directivity factor would vary from 2 to 8 dB (taking 8 dB as the peak factor), a directivity factor of $10 \log_{10} Q(\theta) = 5$ dB was applied to the averaged spectra. The source to receiver distance R was taken to be $d/\sin(70 \text{ deg})$.

3) The efficiency factor of $\eta = 0.005$ was assumed for all of the vehicles. This is a good estimate for large rockets ($T >$ 2.2 MN), but results in overestimates for smaller thrust engines.[9] Note that the Delta has multiple strap-on rockets of relatively small individual thrust (380 kN).

Dimensionless One-Third-OBSPLs

One-third-octave band levels averaged over the 6-dB down period were normalized as

$$\text{dimensionless } \tfrac{1}{3}\text{-OBPWL} = \tfrac{1}{3}\text{-OBSPL} + 10 \log_{10}(4\pi R^2/m^2) - \text{OAPWL} - 5 \text{ dB} \quad (3)$$

where

$$\text{OAPWL} = 10 \log_{10}(\eta \tfrac{1}{2} TV_e/10^{-12} \text{ W}) \text{ dB} \quad (4)$$

The 5.0-dB term on the right-hand side of Eq. (3) is the directivity factor. The OAPWL was estimated using $\eta = 0.005$.

Overall Sound Pressure Levels

Predictions of OASPL vs time are compared to measured levels at the four measurement locations in the first set of Titan IV data. This is the only launch for which trajectory data were available, and the measurement times were coordinated with launch times. OASPL predictions were made using distances

Table 1 Comparison of maximum 1-s averaged OASPLs with predicted values[a]

Vehicle	Actual measurement distance from pad, km	Normalized distance from pad, d/D_e	Maximum 1.0-s averaged OASPL normalized to 1 km, dB	Predicted OASPL at 1 km with $\eta = 0.005$ and $Q = 8$ dB
Scout (185.9 dB,[b] one solid[c])	0.36	420	117.7	122.4
	0.64	740	117.1	
	0.94	1100	117.5	
	1.22	1410	116.0	
Delta (193.1 dB,[b] six solids and liquid core[c])	0.46	400	123.4	129.6 dB
	0.61	530	126.1	
	0.92	800	125.0	
Peacekeeper (191.7 dB,[b] one solid[c])	0.30	210	127.2	128.2 dB
	0.61	420	126.0	
	1.22	840	127.5	
Titan IV (198.8 dB,[b] two solids[c])	0.50	160	136.8	135.3 dB
	12.62	3940	129.5	
	13.58	4240	130.9	
	15.73	4900	131.3	
	0.82	245	140.0	135.3 dB
	2.04	605	137.6	
	3.41	1020	139.7	
	5.79	1725	137.5	
	13.15	3920	135.2	

[a]OASPLs adjusted for spherical spreading to a normalized distance of 1 km from the pad.
[b]Acoustic power.
[c]Number of engines.

R and solid angles θ, calculated from trajectory data, and Eq. (1) integrated over frequency:

$$\frac{p'^2(R,\theta)}{\rho_0 c_0} = \eta \left(\frac{1}{2} TV_e\right) \frac{1}{4\pi R^2} Q(\theta) \tag{5}$$

Data Analysis Results

Maximum OASPLs

Maximum 1.0-s averaged, OASPLs measured at the Scout, Delta, Peacekeeper, and Titan IV locations have been normalized to a distance of 1 km from the pad and are summarized in Table 1. This table is arranged in ascending order of overall thrust. The Delta vehicle has individual engines of smaller thrust than either the single Peacekeeper or Scout engines; the Titan IV has the largest engines. Nozzle exit velocities are approximately the same for the solid engines on all of these vehicles, so that thrust comparisons are equivalent to mechanical power comparisons. Three observations can be made regarding the data in Table 1.

1) Maximum OASPLs are consistently overpredicted for the smaller vehicles when $\eta = 0.005\%$ and an 8-dB peak directivity factor (the maximum derived from the vertical launch data of Cole et al.[5]) are assumed. In the case of the Titan IV, the use of these factors resulted in underestimates of maximum OASPLs.

2) When OASPLs (as measured) are less than 123 dB (one Scout measurement location and several of the Titan IV locations), the maximum OASPL decreases with distance faster than expected on the basis of spherical expansion. Particularly in the case of the Titan IV, where peak one-third-OB frequencies are below 50 Hz, this decrease cannot be attributed to atmospheric absorption.

3) The levels for the second set of Titan IV data, when normalized to a distance of 1 km from the pad, are consistently higher, by roughly 4.0 dB, than those of the first set. Although different instrumentation systems were used, calibration signals were recorded in all cases and it is unlikely that this 4-dB difference is solely from the use of different measurement or analysis systems.

Comparison of OASPL Measurements with Predictions

In Figs. 2 and 3, the first set of Titan IV data are compared with OASPL predictions. (The early overpressure levels indicated in Fig. 2 are misleading, as one-third-octave band Butterworth filtering and a 1.0-s averaging time are not appropriate for characterizing this transient event.) No atmospheric absorption factors were applied in these predictions, as virtually no absorption is expected in the one-third-OBs that control the OASPL for the Titan IV.

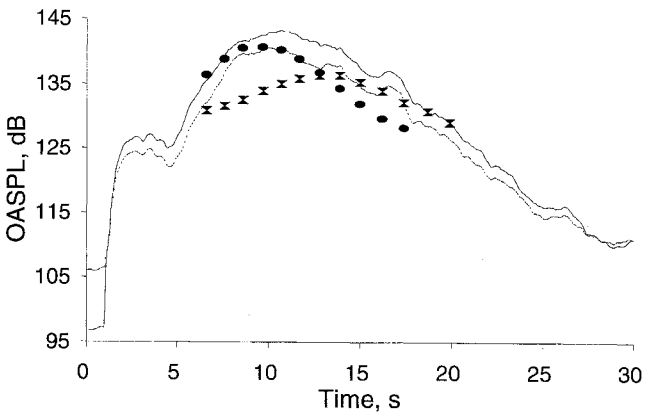

Fig. 2 Comparison of predicted and measured OASPLs vs time 0.5 km from the Titan IV Launch Pad. Curves are sums of 1-s averaged one-third-OBs measured by two different microphones. Ellipses are predictions using vertical launch directivity factors; hourglasses are predictions using horizontal ground test directivity factors.

In the predictions, two different sets of directivity factors were tried. When directivity factors derived from horizontal ground test data (see Fig. 46 in Ref. 5) were used, predicted OASPLs peaked at times substantially later than the measured peak times at all four locations. A single set of the predictions obtained using these horizontal test directivity factors is shown in Fig. 2 (the solid hourglass markers). A peak directivity factor of 5 dB for $50 \leq \theta \leq 55$ deg was used in these predictions.

The use of directivity factors derived from the vertical launch data in Ref. 5 substantially improved the timing and trend comparisons at all four locations, but resulted in overpredictions at the distant locations. A peak directivity factor of 8 dB for $70 \leq \theta \leq 75$ deg was used in this second set of predictions. The overprediction in OASPL at large distances from the pad may be because of the fact that the estimation

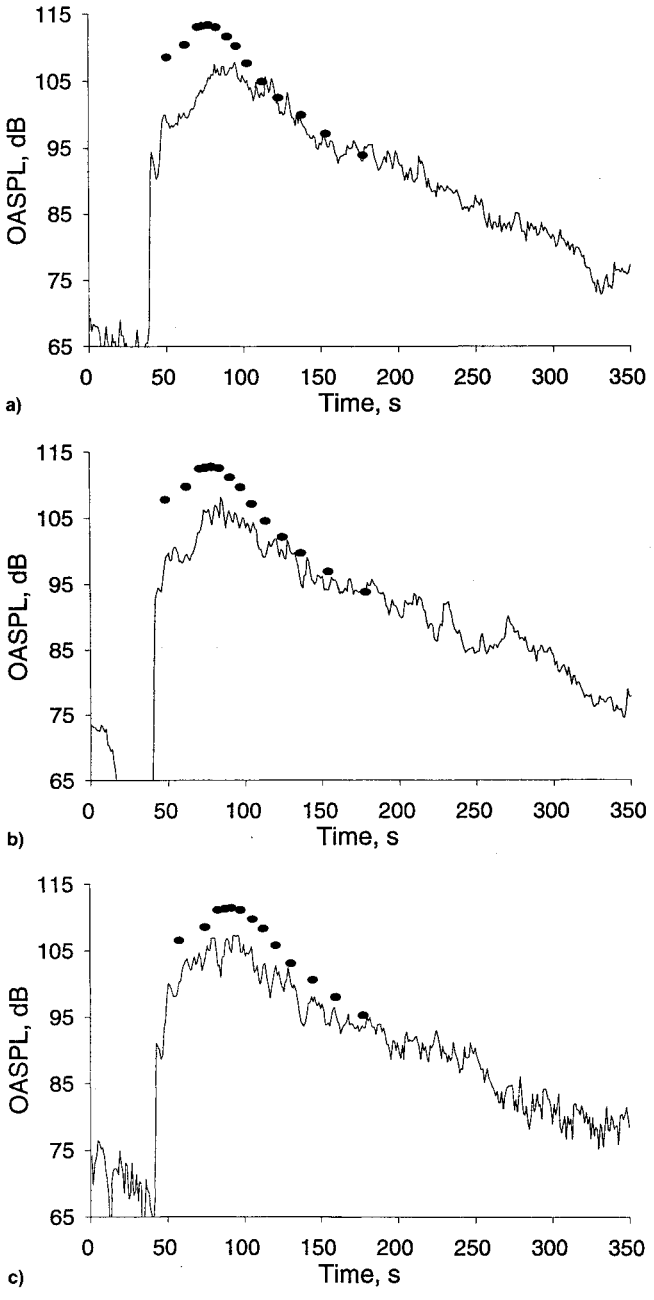

Fig. 3 Comparison of predicted and measured Titan IV OASPLs vs time at these distances from the pad: a) 12.62, b) 13.58, and c) 15.73 km. Solid curves are 1-s averages recorded by real-time analyzer; ellipses are predictions using vertical launch directivity factors.

method does not account for the shift in energy from the low-frequency levels (where the spectrum peaks), to the high frequencies that accompanies nonlinear acoustic propagation.[10,11] When first presented,[12] the predictions shown in Figs. 2 and 3 were 3 dB too high, because the factor of one-half was erroneously omitted in the calculation of mechanical power [see Eq. (4)].

Dimensionless Titan IV One-Third-OBPWLs

Normalized one-third-OBPWL estimates constructed from the first set of Titan IV measurements are given in Fig. 4. (Normalized one-third-OBPWL estimates for the Peacekeeper, Delta, Scout, and the second set of Titan IV data can be found in Ref. 13.) Since the two microphones 0.5 km from the pad were on a tower some distance off the ground (the measurement heights are unknown), the lobing of these spectra is thought to be the result of ground reflections. The average OASPLs (over the 6-dB down period) for these two measurements were 141.6 and 138.7 dB. At the locations 12.62–15.73 km from the pad, the average OASPLs (over the 6-dB down period) ranged from 104.6 to 105.1 dB.

In Fig. 4, no adjustments were made to the one-third-octave sound power estimates to account for atmospheric absorption. In this data, high-frequency SPLs decrease with distance less than is expected on the basis of atmospheric absorption and spherical spreading. Peak low-frequency levels, on the other hand, decrease more than is expected.

Dimensionless PSDs

Dimensionless PSDs estimated from sound pressure spectral densities for the Scout, Delta, Peacekeeper, and Titan IV are shown in Figs. 5–8, respectively. One-third-octave versions of these PSDs can be found in Ref. 13. The use of an acoustic efficiency factor of $\eta = 0.005$ results in normalized PSDs that are too low for the Scout and Delta and too high for the Titan IV [see Eq. (2b) and the OASPL comparisons in Table 1]. With regard to the frequency distribution of the spectra, the Scout and Peacekeeper had single engines so that there was no ambiguity in the parameter (V_e/D_e). In the Delta spectra of Fig. 6, if D_e had been taken equal to D instead of $\sqrt{2}D$, the dimensionless sound power spectral density curves would have moved up by a little more than 1 dB, and have shifted a little to the left on the frequency scale.

Because atmospheric absorption was not accounted for in the construction of the sound power spectral estimates in Figs. 5–8, one would expect the curves to show a consistent de-

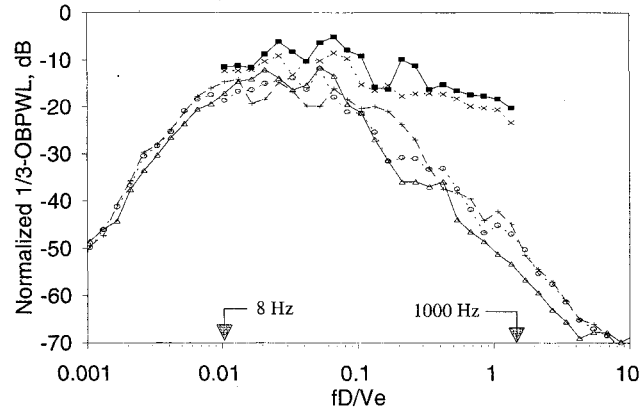

Fig. 4 Normalized Titan IV sound power level estimates in one-third-OBs. Measurement distances and 6 dB down OASPLs: 0.5 km, 141.6 dB, and 0.5 km, 138.7 dB (upper curves); 12.62–15.73 km, 104.6–105.1 dB (lower three curves).

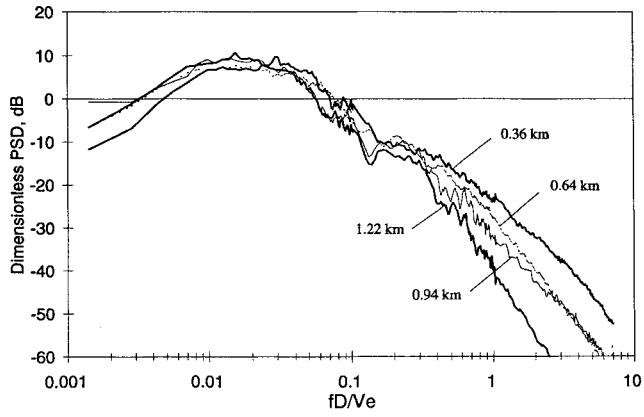

Fig. 5 Dimensionless PSD estimates calculated from the scout data. Measurement distances and OASPLs averaged over the 6-dB down period: 0.36 km, 125.7 dB (top curve); 0.64 km, 118.9 dB; 0.94 km, 115.2 dB; and 1.22 km, 111.5 dB (lower curve).

crease in level with both increasing frequency and increasing measurement distance. It can be seen, however, that such a pattern of decreasing levels consistent with atmospheric absorption is evident only in the spectra derived from measurements where the average OASPL (over the 6-dB down period) was less than 120 dB. The three lower spectra in Fig. 5 (Scout) and the two lowest spectra in Fig. 8 (Titan IV) correspond to average OASPLs of less than 120 dB.

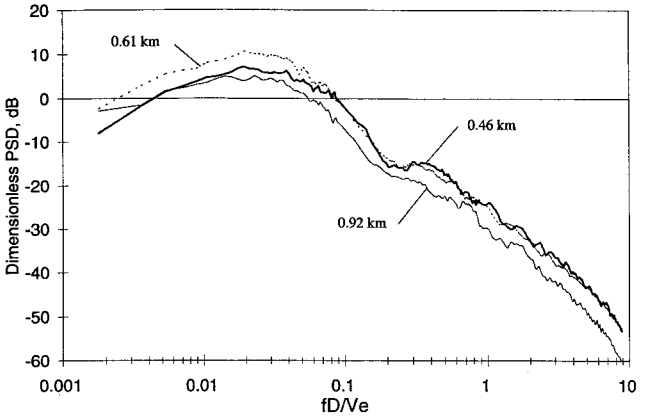

Fig. 6 Dimensionless PSD estimates calculated from the Delta data. Measurement distances and OASPLs averaged over the 6-dB down period: 0.46 km, 128.7 dB; 0.61 km, 128.3 dB; and 0.92 km, 122.8 dB.

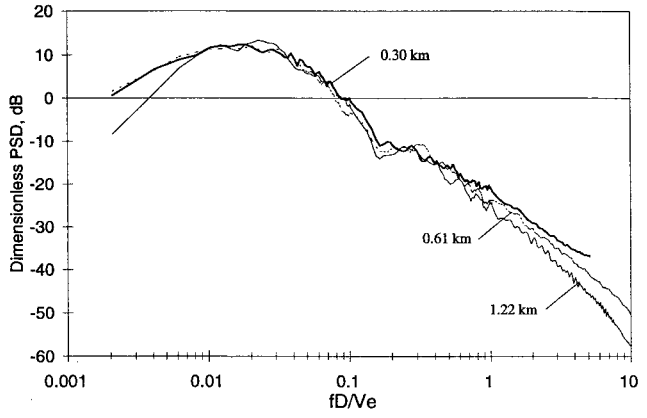

Fig. 7 Dimensionless PSD estimates calculated from the Peacekeeper data. Measurement distances and OASPLs averaged over the 6-dB down period: 0.31 km, 134.9 dB; 0.61 km, 128.2 dB; and 1.22 km, 123.3 dB.

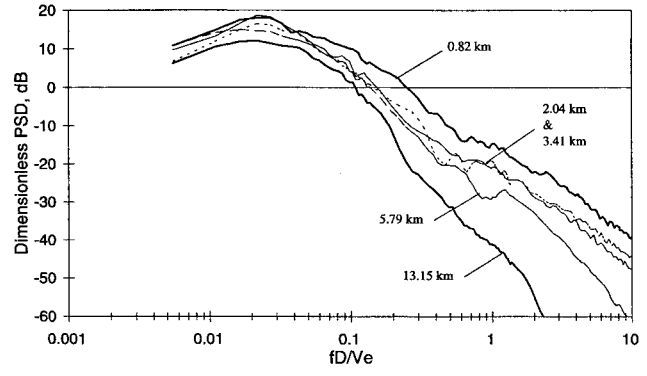

Fig. 8 Dimensionless PSD estimates calculated from the Titan IV data. Measurement distances and OASPLs averaged over the 6-dB down period: 0.82 km, 139.5 dB (top curve); 2.04 km, 129.0 dB, and 3.41 km, 127.1 dB (middle curves); 5.79 km, 119 dB, and 13.15 km, 109.2 dB (lower curves).

The peak frequencies and peak levels (when adjusted for actual efficiencies) in Figs. 5–8 compare well with the dimensionless PSD of Ref. 8. However, at high frequencies, the PSDs in Figs. 5–8 are deficient in energy relative to the widely utilized PSD of Ref. 8. It is not known if linear atmospheric absorption corrections were included in the calculation of the dimensionless sound power spectral densities (from one-third-OBSPLs) in Refs. 5 and 8.

Conclusions

Maximum OASPLs measured at several locations during Peacekeeper, Delta, Scout, and Titan IV launches were normalized to 1.0 km and compared to predictions made assuming an acoustic efficiency of $\eta = 0.005$ and a peak directivity factor of 8 dB. These comparisons indicated that the use of an efficiency factor of $\eta = 0.005$ and a peak directivity factor of 8 dB results in overpredictions for the smaller thrust vehicles, but results in underpredictions in the case of the Titan IV. For OASPLs (1-s averaged) below 123 dB, measured maximum OASPLs decreased with distance faster than expected on the basis of spherical spreading and atmospheric absorption.

OASPLs as a function of time were compared with predictions at four locations during a single Titan IV launch. The use of directivity factors derived from the vertical launch data[5] (instead of directivity factors derived from horizontal ground test data) substantially improved the timing and trend comparisons at all four locations. Dimensionless constant bandwidth, sound power spectral densities estimated from sound pressure spectral densities were presented for each of the Scout, Delta, Peacekeeper, and Titan IV. These PSDs and a set of normalized Titan IV one-third-OBSPLs displayed high-frequency levels that decreased with distance less than is expected on the basis of atmospheric absorption and spherical spreading. Nonlinear propagation effects have been suggested as a possible explanation for the faster than expected decrease in the low-frequency levels that control the OASPL, and the smaller than expected decrease in high-frequency levels, with increasing distance from the pad.

Acknowledgments

The author would like to thank Norman Keegan of The Aerospace Corporation for his support and continued interest in this project and to Harry Himelblau for improving the clarity of the manuscript.

References

[1]McInerny, S. A., "The Broadband Noise Generated by Very High Temperature, High Velocity Exhausts," *Proceedings of the 2nd International Congress on Recent Developments in Air- and Structure-Borne Sound*, edited by M. J. Crocker and P. K. Raju, Vol. 1, Auburn Univ., Auburn, AL, 1992, pp. 59–66.

[2]Von Gierke, H. E., "Types of Pressure Fields of Interest in Acoustical Fatigue Problems," Wright Air Development Center (WADC)–Univ. of Minnesota Conference on Acoustic Fatigue, WADC TR 59-676, March 1961.

[3]McInerny, S. A., "Characteristics and Predictions of Far-Field Rocket Noise," *Noise Control Engineering Journal*, Vol. 38, No. 1, 1992, pp. 5–16.

[4]Potter, R. C., and Crocker, M. J., "Acoustic Prediction Methods for Rocket Engines, Including the Effects of Clustered Engines and Deflected Exhaust Flow," NASA CR-566, Oct. 1966.

[5]Cole, J. N., Von Gierke, H. E., Kyrazis, D. T., Eldred, K. M., and Humphrey, A. J., "Noise Radiation from Fourteen Types of Rockets in the 1,000 to 130,000 Pounds Thrust Range," Wright Air Development Center (WADC) TR 57-354, Dec. 1957.

[6]Cole, J. N., England, R. T., and Powell, R. G., "Effects of Various Exhaust Blast Deflectors on the Acoustic Noise Characteristics of 1000 Pound Thrust Rockets," Wright Air Development Center (WADC) TR 60-6, Sept. 1960.

[7]Van Ert, D., McGregor, H. N., and Hart, P., "624A Scale Model Flame Deflector Program," Martin Marietta Corp., Contract AF 04(695)-54, Denver, CO, Jan. 1963.

[8]Eldred, K., "Acoustic Loads Generated by the Propulsion System," NASA SP-8072, June 1971.

[9]Guest, S. H., "Acoustic Efficiency Trends for High Thrust Boosters," NASA TN D-1999, July 1964.

[10]Pestorius, F. M., and Blackstock, D. T., "Propagation of Finite Amplitude Noise," *Finite-Amplitude Wave Effects in Fluids, Proceedings of the 1973 Symposium*, edited by L. Bjorno, IPC Science and Technology Press Ltd., Surrey, England, UK, 1974, pp. 24–29.

[11]Webster, D., and Blackstock, D. T., "Experimental Investigation of Outdoor Propagation of Finite-Amplitude Noise," NASA Langley Research Center, CR 2992, Hampton, VA, Aug. 1978.

[12]McInerny, S. A., "Spectral and Time Domain Characteristics of the Non-Linear Acoustics Generated by Launch Vehicles," AIAA Paper 93-4384, Oct. 1993.

[13]McInerny, S. A., "Measurement, Characterization and Prediction Problems Associated with Rocket Noise," *Proceedings of the 3rd International Congress on Recent Developments in Air- and Structure-Borne Sound and Vibration*, edited by Malcolm Crocker, Vol. 2, International Scientific Publications, Auburn, AL, 1994, pp. 1231–1238.

HELICOPTER FLIGHT DYNAMICS

The Theory and Application of Flying Qualities and Simulation Modeling

Gareth Padfield, Defence Research Agency, United Kingdom

This new volume provides a comprehensive treatment of the theoretical background to the dynamics of helicopter flight, the development of handling criteria, and new flight test techniques. Flying quality is described from both objective and subjective perspectives, and test results are presented from a variety of different sources including the author's own research experience in the United Kingdom and in collaboration with other government agencies.

It is recommended for graduate and postgraduate students in aerospace engineering and engineers in research laboratories and the manufacturing industry, test pilots and flight test engineers.

Introduction • Helicopter Flight Dynamics–An Introductory Tour • Modelling Helicopter Flight Dynamics: Building a Simulation Model: Introduction and Scope, Formulation of Helicopter Forces & Moments in Level I Modelling, Integrated Equations of Motion, Beyond Level I Modelling • Modelling Helicopter Flight Dynamics: Trim and Stability Analysis • Modelling Helicopter Flight Dynamics: Constrained Stability and Response Analysis • Flying Qualities: Objective Assessment and Criteria Development • Flying

AIAA
American Institute of Aeronautics and Astronautics

Place your order today!
Call 800/682-AIAA

AIAA
textbook
1996 514 pp Cloth
ISBN 1-56347-205-8
AIAA Members $85.95
List Price $99.95
Order #: 05-8(945)*

Publications Customer Service, 9 Jay Gould Ct., P.O. Box 753, Waldorf, MD 20604
FAX 301/843-0159 Phone 800/682-2422 9 a.m. – 5 p.m. Eastern http://www.aiaa.org
Outside the U.S. and Canada, order from Blackwell Science Ltd., United Kingdom, 441865 206 206